Available online at www.sciencedirect.com
SCIENCE DIRECT®
Journal of Solid State Chemistry 177 (2004) 951–959
JOURNAL OF SOLID STATE CHEMISTRY
http://elsevier.com/locate/jssc

Magnetic properties and low temperature X-ray studies of the weak ferromagnetic monoclinic and trigonal chromium tellurides Cr_5Te_8

K. Lukoschus,[a] S. Kraschinski,[a] C. Näther,[a] W. Bensch,[a,*] and R.K. Kremer[b]

[a] *Institut für Anorganische Chemie, Christian-Albrechts-Universität Kiel, Olshausenstr. 40, D-24098 Kiel, Germany*
[b] *Max-Planck-Institut für Festkörperforschung, Heisenbergstr. 1, D-70506 Stuttgart, Germany*

Received 5 June 2003; received in revised form 22 September 2003; accepted 28 September 2003

Abstract

Monoclinic and trigonal Cr_5Te_8 show a transition into the ferromagnetic state with a Curie temperature T_c, which sensitively depends on the actual composition. Monoclinic samples exhibit a lower T_c despite their higher Cr content. This observation is explained on the basis of less effective ferromagnetic superexchange in the monoclinic compounds and the larger number of Cr atoms being antiferromagnetically coupled. Magnetization experiments performed at 5 K demonstrate that the compounds saturate already at rather low magnetic fields. In addition, small values are estimated for the coercitive field H_c as well as for the remanence magnetization both being typical for weak ferromagnetic materials. The values for the saturation magnetization amount to about 72% and 65% for monoclinic and trigonal Cr_5Te_8, respectively. These low values can partially be explained on the basis of antiferromagnetically coupled Cr(III) d^3 centers. An additional spin canting is assumed to fully account for the reduced saturation moments. Above 300 K the susceptibilities follow a Curie–Weiss law with large positive values for the Weiss constant and magnetic moments in accordance with a Cr^{3+} $3d^3$ spin configuration. Low temperature X-ray investigations reveal unusual thermal expansion of the **a** as well as **b** lattice parameters of the monoclinic and of the **a** lattice parameter of the trigonal sample, respectively. Near T_c the slope of the thermal expansions changes significantly.

Keywords: Chromium tellurides; Magnetic properties; Composition dependence of Curie-temperature; Thermal expansion of the structures

1. Introduction

The crystal structures of monoclinic and trigonal Cr_5Te_8 are closely related to the hexagonal NiAs structure type. The metal atom deficient phases are obtained by removing metal atoms from every second metal atom layer in the NiAs structure type in an ordered way. In monoclinic Cr_5Te_8 (m-Cr_5Te_8) the Cr atoms occupy four different crystallographic sites. The resulting ordering of the vacancies is significantly different from the structures of other transition metal chalcogenides with composition M_5X_8 (M= Ti, V; X= S, Se, Te). A slight increase of the tellurium content leads to an order–disorder transition from the monoclinic to a trigonal phase (tr-Cr_5Te_8). In tr-Cr_5Te_8 the Cr atoms are located on four crystallographically different sites leading to the formation of a five-layer superstructure of the CdI_2 type. The transition from the monoclinic to the trigonal phase occurs in a very narrow composition range: monoclinic symmetry is found in the range 59.6–61.5 at% Te ($CrTe_{1.48}$–$CrTe_{1.60}$) [1]. Stoichiometric m-Cr_5Te_8 (61.54 at% Te) is stable at low temperatures whereas the trigonal modification is obtained by quenching the samples from about 1075 K to room temperature [1]. The homogeneity range of tr-Cr_5Te_8 was reported to be about 61.8–62.5 at% Te [2] and the space group for this modification to be $P\bar{3}c1$ [1]. However, as was shown in our previous work the space group of tr-Cr_5Te_8 is rather P-$3m1$ [3]. A slightly different upper phase boundary for tr-Cr_5Te_8 of 63.6(6) at% Te was reported by Viswanathan et al. [4]. Until know only a few studies were performed on m-Cr_5Te_8 and tr-Cr_5Te_8 regarding their physicochemical properties. The pressure dependence of the spontaneous magnetization of Cr_5Te_8 measured at 4.2 K was reported for a trigonal sample with lattice parameters $a = 3.914$ Å and $c = 5.998$ Å [5]. The heat capacities of m-Cr_5Te_8

*Corresponding author. Fax: +4341-880-1520.
E-mail address: wbensch@ac.uni-kiel.de (W. Bensch).

0022-4596/$ - see front matter © 2003 Elsevier Inc. All rights reserved.
doi:10.1016/j.jssc.2003.09.041

and tr-Cr_5Te_8 show an order–disorder transition of m-Cr_5Te_8 to the vacancy ordered Cr_3Te_4 type structure at 815 K [6,7]. The lattice parameters of m-Cr_5Te_8 were given with $a = 13.535$ Å, $b = 7.822$ Å, $c = 11.994$ Å and $\beta = 90.4°$ [6]. In their discussion the authors in Ref. [6] assumed that m-Cr_5Te_8 is isostructural to V_5Te_8, which according to our investigation can be ruled out [3].

Shimada et al. performed photoemission studies on Cr_5Te_8 and concluded that Cr_5Te_8 is an itinerant ferromagnet [8]. We note that the sample investigated by this group showed trigonal symmetry with lattice parameters $a = 3.924$ Å and $c = 6.008$ Å. Recently, the magnetic properties of solid solutions with compositions $(Cr_{1-y}V_y)_5Te_8$ and $(Cr_{1-x}Ti_x)_5Te_8$ were investigated [9–11]. But in all contributions the crystal structures correspond to a CdI_2-type cell and the ratio of Cr:Te was always fixed to 5:8. In addition, no monoclinic samples were studied by the authors and no attention was drawn onto the fact that the actual composition of the samples should sensitively influence the physical properties.

Assuming that divalent Te anions are present the average oxidation state of Cr is 3.2. Using an ionic picture, the compounds can be formulated as $(Cr^{3+})_4(Cr^{4+})Te_8$, with electronic configurations $3d^2$ and $3d^3$ coexisting. This electronic situation is altered changing the stoichiometry from the exact 5:8 ratio for Cr:Te. However, it is highly unlikely that Cr(IV) exists in the presence of Te. As was demonstrated in several contributions Te–Te interatomic separations as large as about 3.8 Å may lead to weak interactions, found, e.g. for ZrSiTe or $TiTe_2$ [12,13]. As established in a preceding work, the Te–Te contacts in both phases are significantly shorter than 3.8 Å thus indicating weak Te–Te interactions. Such weak interactions may reduce the negative charge on the Te anions because the top of the Te *sp* bands, which has some antibonding character, is depopulated and the Te–Te distances are shortened. The existence of short anion–anion contacts may be indicative of an electron transfer from *sp* anion to *d* cation electronic states. In addition, in both phases relatively short Cr–Cr distances are observed suggesting weak bonding between the Cr atoms. Such metal–metal bonds may further reduce the positive charge on the Cr atoms.

In view of this electronic situation an investigation of the magnetic properties of monoclinic and trigonal Cr_5Te_8 particularly as function of actual composition may provide further insight into the bonding properties of these compounds. It can be expected that the physical properties are very sensitive to the actual Cr content and will vary significantly within the narrow composition range in which the crystal structure transforms from monoclinic to trigonal symmetry.

2. Experimental details

2.1. Synthesis

Elemental Cr and Te powders (99.6% and 99.9%) were mixed in the desired ratios and were transferred into dried silica ampoules. The ampoules were evacuated ($\sim 10^{-5}$ mbar) and heated to 400°C at a rate of 100°C/h. After 4 days the temperature was raised to 1000°C at a rate of 5°C/h and after 3 days the ampoules were cooled to room temperature at a rate 100°C/h. The products consisted of black powders and black crystals with a platelet like shape. The samples are stable in air over a long period. The composition of the samples was determined by atomic absorption spectroscopy (AAS).

2.2. Magnetic susceptibility investigations

Between 300 and 600 K magnetic susceptibility measurements were measured with a Faraday balance in an applied field of 1.5 T. Magnetization measurements at 300 K in magnetic fields between 0.1 and 1.5 T showed that ferromagnetic impurities can be neglected. The susceptibility data were corrected for core diamagnetism using Pascal increments.

Low temperature susceptibility measurements between 4 and 300 K were performed in a Quantum Design MPMS SQUID magnetometer on the two samples m-$Cr_{5.016}Te_8$ and tr-$Cr_{4.876}Te_8$ in a field of 0.1 T. Isothermal magnetization was measured up to 7 T at different temperatures between 5 and 200 K on both powders and pressed pellets.

2.3. X-ray studies

X-ray powder patterns were collected at room temperature on a Siemens D5000 diffractometer using monochromatized Cu$K\alpha$ radiation ($\lambda = 1.54056$ Å). Rietveld profile refinements of the powder patterns of all magnetically investigated samples were performed using the FULLPROF program package [14]. The background was modelled with interpolated points. For Cr and Te the isotropic displacement parameters were tied for each group and refined with a freely varying variable. Preferred orientation was treated using the March–Dollase function. A Thompson–Cox–Hastings function with 5 profile parameters was used to model the peak shapes.

Single-crystal X-ray work was done using a Nonius CAD-4 four-circle diffractometer (monochromatized Mo$K\alpha$ radiation, $\lambda = 0.7107$ Å) equipped with a cooling device from Oxford instruments. The lattice parameters were determined between 320 and 100 K. Because no single crystals suitable for the X-ray work could be selected from the product of the monoclinic sample with composition $Cr_{5.016}Te_8$ the low temperature experiments were performed on a crystal with composition

$Cr_{4.98(2)}Te_8$ very near to the 5:8 composition. We note that at lower temperatures a significant broadening of the reflections occur. Nevertheless, a structure refinement was performed for one data set (160 K) of the monoclinic sample to get an impression which interatomic distances are mainly affected by the anisotropic changes of the lattice parameters. The raw intensities were treated in the usual way and structure refinement was done against F^2 using SHELXL-97 [15]. The occupancy of Cr4 position is low and the occupancy of this position was refined with isotropic displacement factors whereas for all other atoms anisotropic displacement parameters were allowed. The main results of the structure refinements (300 and 160 K) and some technical details are summarized in Table 1.

3. Results

3.1. Magnetic properties in the high temperature region

In Fig. 1 the temperature dependence of the magnetic susceptibilities between 300 and 600 K of m-$Cr_{5.016}Te_8$ and tr-$Cr_{4.876}Te_8$ are displayed. The numerical results are summarized in Table 2. The fit with the Curie–Weiss law yields an effective magnetic moment of 3.86(2) μ_B/Cr for m-Cr_5Te_8 and 3.87(2) μ_B/Cr for tr-Cr_5Te_8. Both effective moments are near the spin only value expected for a Cr^{3+} with a d^3 electronic configurations. The values for the paramagnetic Curie temperature θ are found with 196(1) and 235(1) K for m-$Cr_{5.016}Te_8$ and tr-$Cr_{4.876}Te_8$, respectively, indicating considerable predominant ferromagnetic exchange interactions.

We note that fitting the data with a modified Curie–Weiss law including contributions from temperature-independent paramagnetism (TIP) always yielded unrealistic negative values for the TIP. This is not surprising since the density of states at the Fermi level is low [8]. Hence, one cannot expect an appreciable Pauli paramagnetic contribution to the susceptibility.

We further draw particular attention to the finding that the trigonal sample with the lower Cr content exhibits the higher value for θ and for T_c (see below), indicating more effective ferromagnetic exchange.

3.2. Magnetic properties in the low temperature region

The temperature dependence of the susceptibilities for m-$Cr_{5.016}Te_8$ and tr-$Cr_{4.876}Te_8$ recorded between 300

Table 1
Selected technical details of data acquisition and refinement results for monoclinic $Cr_{4.98(2)}Te_8$ obtained at 300 K and at 160 K

	300 K	160 K
a (Å)	13.539(3)	13.5712(6)
b (Å)	7.8096(14)	7.8286(5)
c (Å)	11.987(2)	11.8813(11)
β (deg)	90.156(14)	90.140(6)
V (Å^3)	1267.4(4)	1262.31(15)
$2\theta_{max}$ (deg)	60	60
No. unique reflections	985	976
R_1 (all reflections)	0.0467	0.0802
wR_2 (all reflections)	0.0917	0.1274
GOF	1.008	1.029
δF (e/Å^3)	1.76/−2.99	2.36/−4.25

Estimated standard deviations are given in parentheses.

Table 2
Magnetic data for m-Cr_5Te_8 and tr-Cr_5Te_8

	$Cr_{5.016}Te_8$	tr-$Cr_{4.876}Te_8$
Temp. range (K)	300–600	300–600
μ/Cr (μ_B)	3.86(1)	3.87(1)
θ (K)	196(1)	236(1)
Temp. range (K)	330–600	330–600
μ/Cr (μ_B)	3.81(1)	3.80(1)
θ (K)	202(1)	241(1)
Temp. range (K)	355–600	355–600
μ/Cr (μ_B)	3.81(1)	3.80(1)
θ (K)	201(1)	242(1)

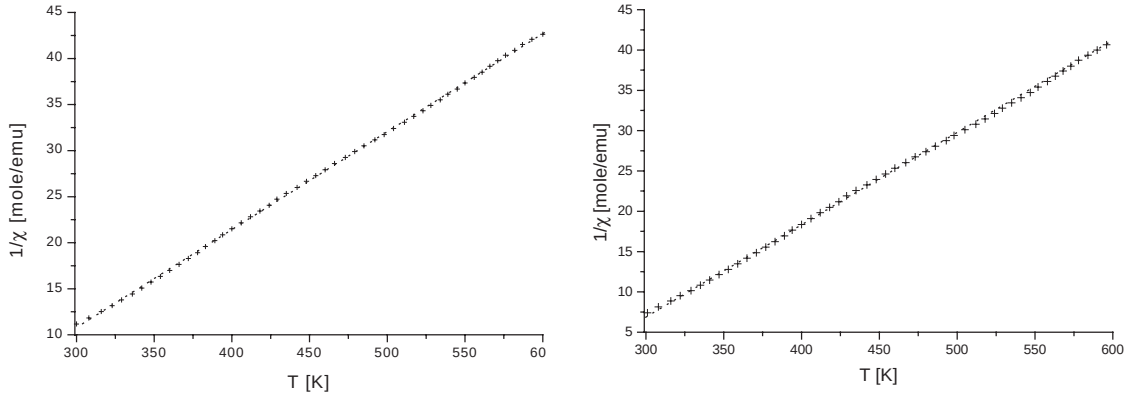

Fig. 1. The inverse magnetic susceptibilities between 300 and 600 K for m-Cr_5Te_8 (left) and tr-Cr_5Te_8 (right). The dotted lines are the results of a Curie–Weiss fit.

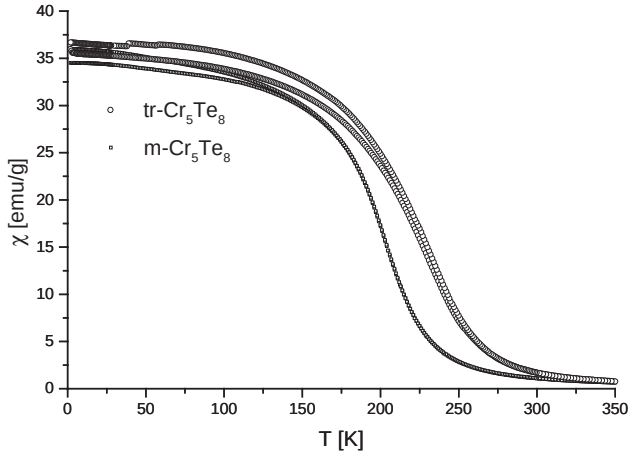

Fig. 2. The magnetic susceptibilities below 300 K for m-Cr_5Te_8 and tr-Cr_5Te_8 measured with 1 T.

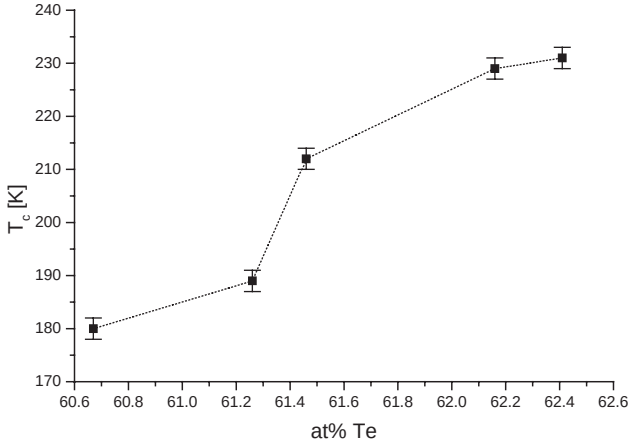

Fig. 3. The dependence of the Curie temperature T_c from composition of the chromium tellurides. The dotted line is a guide for the eyes.

and 4 K are shown in Fig. 2. The extrapolated Curie temperatures T_c are 190 K for m-$Cr_{5.016}Te_8$ and 245 K for tr-$Cr_{4.876}Te_8$, both being close to the paramagnetic Curie temperature θ obtained from a the fit of the high temperature (see above). The variation of T_c with composition is displayed in Fig. 3. With increasing Te content T_c raises and close to the monoclinic to trigonal structural phase transition a jump like increase is observed.

For trigonal Cr_5Te_8 samples T_c values were reported as 220 [8] and 223 K [11] (see Introduction).

Hysteresis loops taken on polycrystalline sample between 5 and 300 K are displayed in Figs. 4 and 5. Below 200 K the magnetization strongly increases at very low fields reaching saturation above 0.2 T. The saturation magnetization M_{sat} is 10.2 μ_B for m-$Cr_{5.016}Te_8$ and 8.65 μ_B for tr-$Cr_{4.876}Te_8$. Both values are significantly smaller than is possible for a full ferromagnetic alignment (14.1 μ_B for m-$Cr_{5.016}Te_8$ and 13.3 μ_B for tr-$Cr_{4.876}Te_8$) of the magnetic dipoles. For the remanent magnetization M_r values of 6.62 and 6.92 μ_B are estimated for the monoclinic and trigonal sample, respectively. The shape of the curves for m-Cr_5Te_8 and tr-Cr_5Te_8 differ and may be attributed to the different crystallite sizes in the two investigated samples. Recently, Kanomata et al. reported saturation measurements performed at 4.2 K on a trigonal Cr_5Te_8 sample [5] (note also the remarks in the Introduction), but no saturation was observed up to about 9 kOe and the data presented in the paper differs significantly from our results. The estimated magnetic moment was found to be 1.2 μ_B per Cr atom [5].

3.3. X-ray diffraction studies

A comparison of the crystal structure of m-$Cr_{4.98}Te_8$ with Cr-richer monoclinic samples reveals that the two sites in the partially occupied layers are successively depleted. This observation indicates that with decreasing Cr content the two positions 4*b* and 8*e* are depopulated and for $Cr_{4.98}Te_8$ the site occupation factors (sof) for 4*b* and 8*e* are 0.17(1) and 0.07(1), respectively. Note, that for a Cr richer monoclinic sample m-$Cr_{5.10}Te_8$ the sofs for the two sites were refined to 0.217(1) and 0.057(2) [3].

For m-$Cr_{4.98}Te_8$ and tr-Cr_5Te_8 the evolution of the lattice parameters with temperature was recorded between 330 and 100 K (see Figs. 6 and 7). For m-$Cr_{4.98}Te_8$ the **c**-axis contracts linearly with decreasing temperature. In contrast, **a** and **b** grow when the temperature is lowered, and both exhibit a nearly linear increase down to about $\approx$225 K (Fig. 6). Below this temperature region the slope changes and a second regime with linear behavior is observed down to about 140 K. Below this temperature the cell parameters reach a plateau extending to 100 K. For the first temperature region 330–230 K an expansion of the **a** and **b** lattice parameters of 1.6×10^{-4} and 9.6×10^{-5} Å/K is obtained, between 230 and 140 K the values are 3.1×10^{-4} and 1.8×10^{-4} Å/K. The contraction of the **c** lattice parameter over the whole temperature range amounts to -6.8×10^{-4} Å/K. The overall contraction of the unit cell volume amounts to about 8 Å^3, i.e. about 0.7%, emphasizing the *open* character of the structure Within error bars the monoclinic β angle remains constant. We note that the unit cell volume exhibits a linear decrease over the whole temperature range. A change of the slope at $\approx$225 K is not visible (see Fig. 6).

The variation of the unit cell parameters of the trigonal modification exhibits a similar temperature dependence (Fig. 7). The **a** parameter starts to increase when the temperature is lowered and the **c** parameter contracts with decreasing temperature. There are again two regimes with different slopes. A linear behavior is obvious for both axes down to about 250 K. At this temperature the slope changes and a second regime down to 160 K can be discerned. Below 160 K both axes reach a plateau with no significant alterations down to

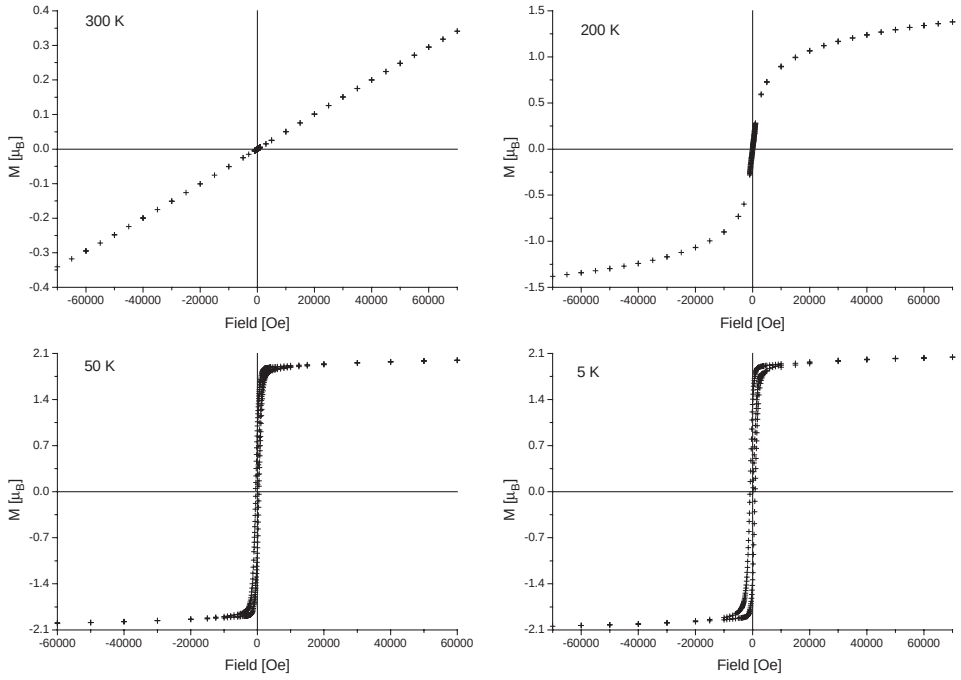

Fig. 4. The magnetization vs. field for m-Cr_5Te_8 measured at different temperatures. Note: the value of M is given for 1 Cr atom.

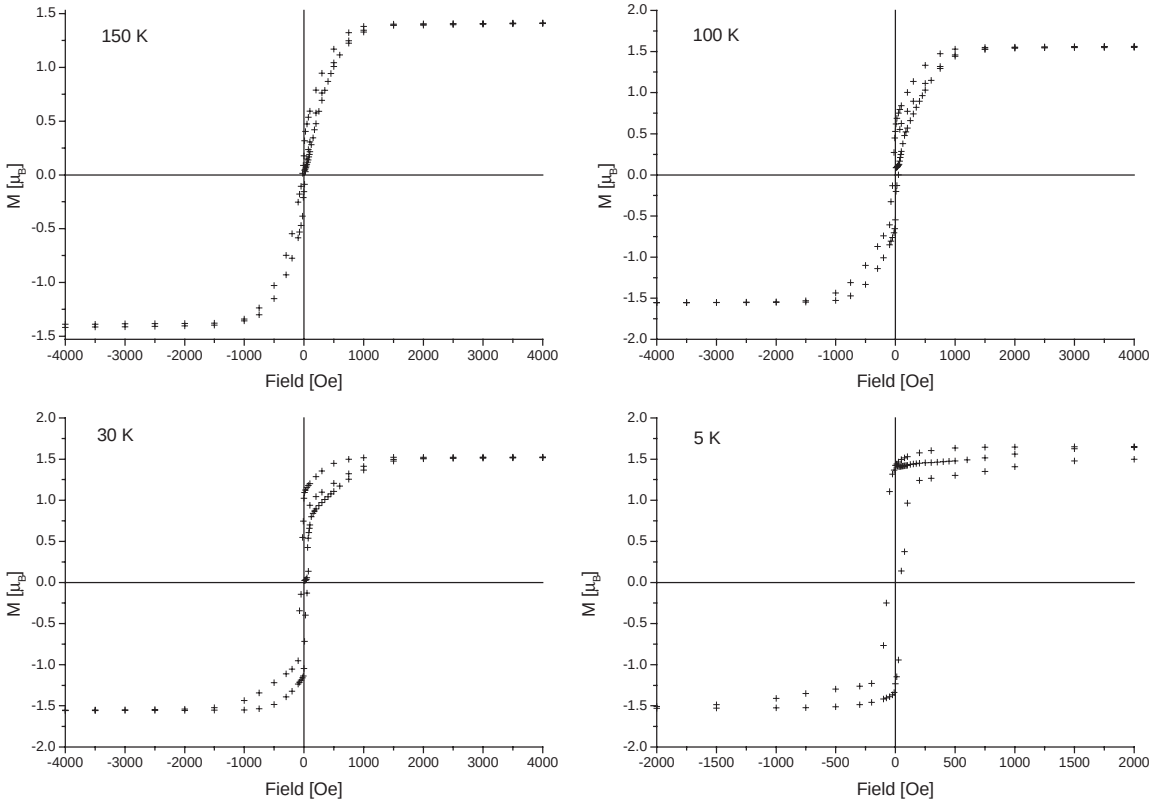

Fig. 5. The magnetization vs. field for tr-Cr_5Te_8 measured at different temperatures. Note: the value of M is given for 1 Cr atom.

100 K. For the **a** parameter the expansion amounts to 9.5×10^{-5} and 1.6×10^{-4} Å/K for the two regions and for the **c** parameter the values are -5.6×10^{-4} and $-8.4\,10^{-4}$ Å/K.

In contrast to the monoclinic sample, the evolution of the unit cell volume with temperature shows a clear deviation from linearity at around 250 K with slopes of -1.3×10^{-2} and -2.1×10^{-2} Å^3/K above and below this

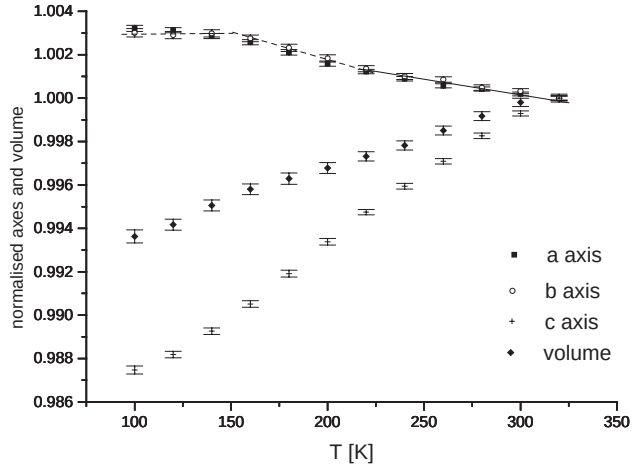

Fig. 6. Variation of the normalized lattice parameters ($a(T)/a(330\,\mathrm{K})$; $b(T)/b(330\,\mathrm{K})$; $c(T)/c(330\,\mathrm{K})$) and of the normalized unit cell volume ($V(T)/V(330\,\mathrm{K})$) of m-Cr_5Te_8 (the angle β shows no significant variation). Note: the different lines joining the symbols are only guides for the eyes.

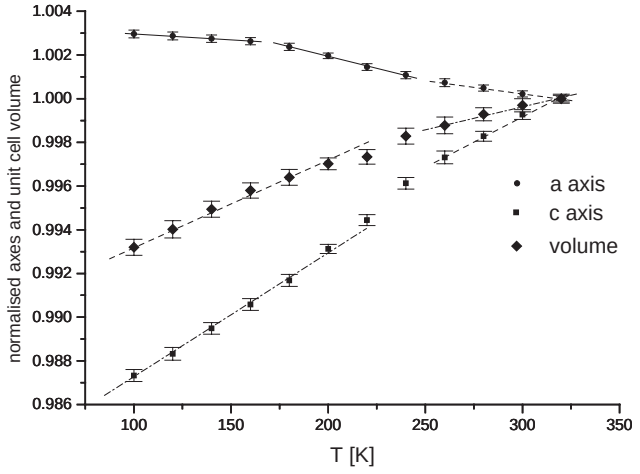

Fig. 7. Variation of the normalized lattice parameters ($a(T)/a(330\,\mathrm{K})$; $c(T)/c(330\,\mathrm{K})$) and of the normalized unit cell volume ($V(T)/V(330\,\mathrm{K})$) of tr-Cr_5Te_8. Note: the different lines joining the symbols are only guides for the eyes.

temperature regime, respectively. Over the whole temperature range the unit cell volume shrinks by about $4.3\,\mathrm{Å}^3$ (0.7%).

4. Discussion

For a discussion of the results we briefly recall the main features of the crystal structures of m-Cr_5Te_8 and tr-Cr_5Te_8 (see Fig. 8) [3]. In both compounds the Cr atoms are in an octahedral environment of Te anions. Within the layers the $CrTe_6$ octahedra share common edges. In m-Cr_5Te_8 the Cr2 and Cr3 atoms are in the fully occupied metal atom layers whereas Cr1 and Cr4

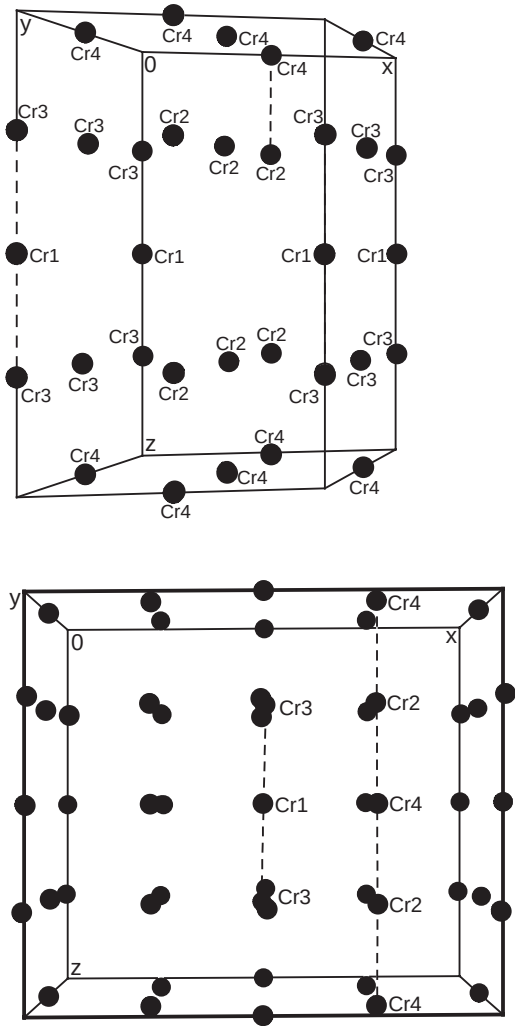

Fig. 8. : The arrangement of the Cr atoms within the unit cell of m-Cr_5Te_8 (bottom) and of trigonal Cr_5Te_8 (top). The Te atoms are omitted for clarity.

are located in the metal deficient layers. The Cr1 and Cr3 as well as the Cr2 and Cr4 centered octahedra share common faces and relatively short Cr–Cr separations parallel to the crystallographic c-axis result (m-$Cr_{4.98}Te_8$: 3.059(1) and 3.000(1) Å). The other Cr–Cr distances are longer and amount to ≈ 3.8 Å. The positions Cr1 and Cr4 are statistically occupied and infinite Cr–Cr atom chains parallel to the c-axis cannot form. According to the occupancy derived from X-ray diffraction results for the full and metal deficient layers the composition formula may be written as $Cr_4[Cr_{1.016}\square_{2.984}]Te_8$ ($\square$ denotes vacancies).

In tr-Cr_5Te_8 two crystallographically different Cr atoms (Cr2 and Cr3) are located in the fully occupied layers. The Cr atoms in the metal deficient layers (Cr1 and Cr4) are distributed over two different sites, with a significantly higher abundance on site Cr1. The Cr2 and Cr4 as well as the Cr1 and Cr3 centered octahedra share common faces and as in the monoclinic modification,

short Cr–Cr distances result (Cr2–Cr4: 3.018(1) Å, Cr1–Cr3: 3.047(1) Å). The final stacking sequence of the metal atoms parallel to the *c*-axis can be represented by the sequence **abcba** (see Fig. 8) and the structure can be regarded as a five-layer superstructure of the CdI_2 structure type. Note that the $Cr1Te_6$ octahedra in one of the metal deficient layers are isolated and these are only connected to the $Cr3Te_6$ octahedra via common faces. As in m-Cr_5Te_8 four Cr atoms occupy the sites in the full metal atom layers and 0.876 Cr are in the metal deficient layers and the formula could be given as $Cr_4[Cr_{0.876}\square_{3.124}]Te_8$.

In the high temperature regime the magnetic susceptibilities of both compounds follow a Curie–Weiss behavior with effective magnetic moments per Cr atom consistent with the spin only value for Cr^{3+} (d^3), supporting the conclusion suggested in our previous work, that Te^{2-} donates electron density to the Cr centers thus stabilizing the Cr(III) oxidation state. In an ionic picture m-$Cr_{5.016}Te_8$ may be written as $[Cr^{3+}]_{4.064}[Cr^{4+}]_{0.952}[Te^{2-}]_8$ and tr-$Cr_{4.876}Te_8$ as $[Cr^{3+}]_{3.504}[Cr^{4+}]_{1.372}[Te^{2-}]_8$. Formally the tellurides then are mixtures of Cr^{3+} (d^3) and Cr^{4+} (d^2) cations, and the expected effective moments μ_{eff}/Cr are 3.70 and 3.61 μ_B/Cr for the monoclinic and trigonal samples, respectively. These values are about 4.4% and 6% smaller than the spin only value for Cr^{3+} with a d^3 configuration ($S = 3/2$). As experimentally found, lower values for the effective magnetic moments are obtained when the fitted range is extended to higher temperatures (see Table 1). Note that μ_{eff}/Cr for most chromium chalcogenides reported in the literature varies over a wide range even for compounds with precise valency [16–23]. Hence it is not straightforward to deduce the oxidation state of the Cr atoms from an analysis of the experimental magnetic moments alone. The Cr^{4+} (d^2) ion is a Jahn–Teller ion but no significant distortions of the $CrTe_6$ octahedra were observed [3].

The paramagnetic Curie temperatures are positive and the magnitudes suggest strong ferromagnetic interactions. According to Kanamori and Goodenough two different exchange contributions must be taken into account to explain the observed magnetic properties [24–27]. The direct Cr^{3+}–Cr^{3+} interaction involves the two t_{2g} orbitals at the two Cr atoms leading to antiferromagnetic exchange. The magnitude strongly depends on the Cr–Cr interatomic separation. A critical distance R_c of about 3.5 Å was reported below which direct exchange interactions can be expected [28]. Ferromagnetic superexchange occurs on the Cr sublattice via 90° Cr–Te–Cr σ/π bonding which links a half-filled t_{2g} (π) on one Cr with an empty e_g (σ) level on the other. Large deviations from the 90° angle weakens the ferromagnetic exchange. Whether a compound exhibits ferromagnetic or antiferromagnetic interactions depends on the detailed geometric configuration such as the Cr–Cr distance and the Cr–Te–Cr angle.

In the compounds short Cr–Cr distances are observed between Cr atoms in the octahedra which share common faces (see above). Within the full and partially depleted metal atom layers the Cr–Cr distances are found between 3.75 and 3.93 Å and thus are too large for direct exchange interactions. In the monoclinic sample the Cr–Te–Cr angles are found between 87.1° and 97.3° in the full layers. They range from 90.3° to 94.4° in the metal deficient layers. In the trigonal compound the analogous angles are between 87.9° and 95.9° and between 90.7° and 93.5°, respectively. In both compounds the angles are close to 90° and ferromagnetic superexchange is favored. It appears to be enhanced in the trigonal samples as the angles are closer to 90°.

Without a detailed knowledge of the spin structures one can only speculate why the experimental M_{sat} is significantly smaller than expected for a full alignment of all magnetic dipoles. Obviously, the Cr atoms located in the octahedra sharing common faces have a Cr neighbor at a short distance of about 3 Å favoring antiferromagnetic interaction. If these Cr atoms are not considered about 2.98 Cr atoms in m-$CrTe_8$ and 3.15 Cr atoms in tr-Cr_5Te_8 can contribute to the ferromagnetic long-range order. The expected values for M_{sat} are then 8.94 μ_B for m-$Cr_{5.016}Te_8$ and 9.45 μ_B for tr-Cr_5Te_8 which are close to the experimental data. We note that for all chromium tellurides in the composition range CrTe to Cr_2Te_3 investigated so far the observed ordered magnetic moments derived from saturation magnetization are smaller than the moments calculated using an ionic model. These deviations have been assigned to spin canting [29–34], non-collinear spin arrangement [35], or a canted antiferromagnetism [36].

The composition dependence of T_c indicates larger values for the samples with lower Cr content. This may be attributed to the increasing number of Cr atoms that do not participate in antiferromagnetic coupling. In addition, ferromagnetic exchange is more effective when Cr–Te–Cr angles approach 90° as it is the case on going from m-Cr_5Te_8 to tr-Cr_5Te_8. We note that for ferromagnetic Cr_3Te_4 T_c strongly depends on the actual composition and values between 315 K and about 350 K were reported [29,35–42].

The low temperature X-ray experiments yield unusual results. For the monoclinic sample the **a** and **b** lattice parameters increase below 300 K (compare Fig. 6). Near T_c both axes show a significant deviation from a linear behavior and the growth is even more pronounced than far above T_c. In contrast, the **c** lattice parameter exhibits a smooth decrease over the whole temperature range. The unit cell volume contracts with a moderate deviation from a linear behavior near T_c. For the trigonal sample the **c** lattice parameter decreases and

Table 3
Selected interatomic distances (Å) and angles (deg) for monoclinic $Cr_{4.98(2)}Te_8$ obtained at 300 and 160 K

	300 K		160 K
Cr(1)–Te(3)	2.7117(4)4 ×		2.6930(9)
Cr(1)–Te(2)	2.7412(7)2 ×		2.7455(12)
⟨Cr(1)–Te⟩	2.722		2.711
δ	0.0295		0.0525
Cr(2)–Te(1)	2.6782(8)2 ×		2.686(2)
Cr(2)–Te(3)	2.7075(6)2 ×		2.7167(8)
Cr(2)–Te(2)	2.7561(9)2 ×		2.740(2)
⟨Cr(2)–Te⟩	2.714		2.714
δ	0.0779		0.054
Cr(3)–Te(1)	2.6802(11)		2.689(3)
Cr(3)–Te(3)	2.7213(8)2 ×		2.713(3)
Cr(3)–Te(3)	2.7279(8)2 ×		2.715(3)
Cr(3)–Te(2)	2.7561(12)		2.741(3)
⟨Cr(3)–Te⟩	2.722		2.714
δ	0.0759		0.052
Cr(4)–Te(1)	2.6537(4)2 ×		2.6633(9)
Cr(4)–Te(3)	2.6796(6)2 ×		2.7036(8)
Cr(4)–Te(2)	2.7540(5)2 ×		2.7253(9)
⟨Cr(4)–Te⟩	2.696		2.697
δ	0.1003		0.062
Cr(1)–Cr(3)	3.0527(11)		3.004(3)
Cr(2)–Cr(4)	2.9990(5)		2.9716(3)
Cr(4)–Te(1)–Cr(4)	94.74(2)	Cr(4)–Te(1)–Cr(4)	94.59(4)
Cr(2)–Te(1)–Cr(2)	86.43(4)	Cr(2)–Te(1)–Cr(2)	88.22(11)
Cr(2)–Te(1)–Cr(3)	89.92(2)	Cr(2)–Te(1)–Cr(3)	91.07(6)
Cr(4)–Te(2)–Cr(4)	90.296(19)	Cr(4)–Te(2)–Cr(4)	91.80(4)
Cr(1)–Te(2)–Cr(4)	90.643(16)	Cr(4)–Te(2)–Cr(1)	91.44(3)
Cr(3)–Te(2)–Cr(2)	93.97(2)	Cr(2)–Te(2)–Cr(3)	93.70(6)
Cr(3)–Te(2)–Cr(2)	93.872(18)	Cr(3)–Te(2)–Cr(2)	93.57(5)
Cr(2)–Te(2)–Cr(2)	97.42(2)	Cr(2)–Te(2)–Cr(2)	96.56(4)
Cr(4)–Te(3)–Cr(1)	92.898(15)	Cr(1)–Te(3)–Cr(4)	93.07(3)
Cr(2)–Te(3)–Cr(3)	88.31(3)	Cr(3)–Te(3)–Cr(2)	89.86(9)
Cr(3)–Te(3)–Cr(3)	91.675(17)	Cr(3)–Te(3)–Cr(3)	92.35(3)
Cr(2)–Te(3)–Cr(3)	95.88(3)	Cr(2)–Te(3)–Cr(3)	94.86(9)

Estimated standard deviations are given in parentheses. δ (delta): difference between largest and shortest Cr–Te bond length.

the **a**-axis increases on lowering the temperature (see Fig. 7). The unit cell volume shrinks and the cell parameters as well as the unit cell volume show a non-linear behavior near T_c. Comparing the structural data obtained at 300 K and at 160 K several alterations are obvious. The Cr–Cr distances across the face-sharing $CrTe_6$ octahedra are reduced from 3.0527(11) and 2.9990(5) Å to 3.004(3) and 2.9716(3) Å at 160 K due to the reduction of the **c** parameter (see Table 3). The shortening of the Cr–Cr distances indicates a stronger Cr–Cr bonding interaction. The average Cr–Te bond lengths are only slightly affected, whereas the distortion expressed as the difference between the longest and shortest Cr–Te distance increases for $Cr(1)Te_6$ and decreases for the other $CrTe_6$ octahedra when the temperature is lowered (Table 3). The angles Te–Cr–Te show also some remarkable changes within the planes perpendicular to the *c*-axis (Table 3). This leads to an expansion of the **a** and **b** parameters in the monoclinic sample. We are convinced that the same alterations occur in the trigonal structure. In m-Cr_5Te_8 the angles Cr–Te–Cr come closer to 90° thus supporting ferromagnetic superexchange to become more effective. We note that depending on the nature of the dominating exchange mechanism an anomalous thermal expansion or contraction of the lattice parameters as well as of the unit cell volume has been reported for different Cr tellurides and selenides [43–49].

In summary, monoclinic and trigonal Cr_5Te_8 are ferromagnetic materials. Their Curie temperatures T_c sensitively depend on the actual composition. Samples with the lower Cr content exhibit higher T_c's. This observation can be understood on the basis of the crystal structures. A larger amount of isolated Cr atoms are found in Cr-depleted samples because the reduction of the Cr content removes Cr atoms from $CrTe_6$ octahedra sharing common faces with neighbors.

Neutron scattering experiments are scheduled to determine the magnetic structure. Knowledge of the spin arrangement is essential for an understanding of the low temperature magnetic properties.

Acknowledgments

Financial support by the State of Schleswig-Holstein is gratefully acknowledged. We thank Mrs. E. Brücher who conducted the magnetic measurements in the low temperature region.

References

[1] H. Ipser, K.L. Komarek, K.O. Klepp, J. Less-Common Met. 92 (1983) 265.
[2] H. Ipser, K.O. Klepp, K.L. Komarek, Monh. Chem. 111 (1980) 761.
[3] W. Bensch, O. Helmer, C. Näther, Mater. Res. Bull. 32 (1997) 305.
[4] R. Viswanathan, M. Sai Baba, T.S. Lakshmi Narasimhan, R. Balasubramanian, D. Darwin Albert Raj, C.K. Mathews, J. Alloys Compds. 206 (1994) 201.
[5] T. Kanomata, Y. Sugawara, K. Kamishima, H. Mitamura, T. Goto, S. Ohta, T. Kaneko, J. Magn. Magn. Mater. 177–181 (1998) 589.
[6] T. Tsuji, K. Ishida, Thermochim. Acta. 253 (1995) 11.
[7] T. Tsuji, T. Kato, K. Naito, J. Nucl. Mater. 201 (1993) 120.
[8] K. Shimada, T. Saitoh, H. Namatame, A. Fujimori, S. Ishida, S. Asano, M. Matoba, S. Anzai, Phys. Rev. B 53 (1996) 7673.
[9] K. Hatakeyama, S. Anzai, H. Yoshida, T. Kaneko, S. Abe, S. Ohta, J. Phys. Soc. Jpn. 71 (2002) 2526.
[10] K. Hatakeyama, T. Kaneko, S. Abe, H. Yoshida, Y. Nakagawa, S. Anzai, J. Phys. Soc. Jpn. 71 (2002) 1605.
[11] K. Hatakeyama, A. Takase, S. Anzai, H. Yoshida, T. Kaneko, S. Abe, S. Ohta, Jpn. J. Appl. Phys. 39 (Suppl. 39-1) (2000) 507.

[12] W. Bensch, O. Helmer, M. Muhler, H. Ebert, M. Knecht, J. Phys. Chem. 99 (1995) 3326.
[13] J. Rouxel, M. Evain, Eur. J. Solid State Inorg. Chem. 31 (1994) 683.
[14] J. Rodriguez-Carvajal, Program FullProf, Version 3.5, 1997.
[15] G.M. Sheldrick, SHELXL-97, Program for the Refinement of Crystal Structures, University of Göttingen, 1997.
[16] T. Ohtani, S. Onoue, Mater. Res. Bull. 21 (1986) 69.
[17] M. Rosenberg, A. Knülle, H. Sabrowsky, Chr. Platte, J. Phys. Chem. Solids 43 (1982) 87.
[18] S. Jobic, F. Bodenan, G. Ouvrard, E. Elkaim, J.P. Lauriat, J. Solid State Chem. 115 (1995) 165.
[19] S. Yuri, S. Ohta, S. Anzai, M. Aikawa, K. Hatakeyama, J. Magn. Magn. Mater. 70 (1987) 215.
[20] A. Lafond, A. Meerschaut, J. Rouxel, J.L. Tholence, A. Sulpice, Phys. Rev. B 52 (1995) 1112.
[21] P. Vaqueiro, A.V. Powell, A.I. Coldea, C.A. Steer, I.M. Marshall, S.J. Blundell, J. Singleton, T. Ohtani, Phys. Rev. B 64 (2001) 132402.
[22] A. Hayashi, Y. Ueda, K. Kosuge, M. Murata, H. Asano, N. Watanabe, F. Izumi, J. Solid State Chem. 67 (1987) 346.
[23] J.H. Zhang, T.L.T. Birdwhistell, C.J. O'Connor, Solid State Commun. 74 (1990) 443.
[24] J.B. Goodenough, Phys. Chem. Solids 6 (1958) 287.
[25] J.B. Goodenough, J. Phys. Rev. 100 (1955) 564.
[26] J. Kanamori, J. Phys. Chem. Solids 10 (1959) 87.
[27] J.B. Goodenough, J. Phys. Chem. Solids 30 (1969) 261.
[28] R.J. Bouchard, P.A. Russo, A. Wold, Inorg. Chem. 4 (1965) 685.
[29] A.F. Andresen, Acta. Chem. Scand. 24 (1970) 3495.
[30] A.F. Andresen, Acta. Chem. Scand. 17 (1963) 1335.
[31] T. Hamasaki, T. Hashimoto, Y. Yamaguchi, H. Watanabe, Solid State Commun. 16 (1975) 895.
[32] E.F. Bertaut, G. Roult, R. Aleonard, R. Pauthenet, M. Chevreton, R. Jansen, J. Phys. (Paris) 25 (1964) 582.
[33] W.J. Takei, D.E. Cox, G. Shirane, J. Appl. Phys. 37 (1966) 973.
[34] B. Lambert-Andron, N.P. Grazhdankina, C. Vettier, J. Phys. (Paris) 39 (1978) L43.
[35] J. Dijkstra, H.H. Weitering, C.F. van Bruggen, C. Haas, R.A. deGroot, J. Phys.: Condens. Matter 1 (1989) 9141.
[36] K. Sato, Y. Aman, H. Hongu, J. Magn. Magn. Mater. 104–7 (1992) 1947.
[37] S. Ohta, J. Phys. Soc. Jpn. 54 (1985) 1076.
[38] D. Babot, M. Chevreton, J. Solid State Chem. 8 (1973) 166.
[39] M. Yuzuri, M. Sato, J. Magn. Magn. Mater. 70 (1987) 221.
[40] K. Ozawa, T. Yoshimi, M. Irie, S. Yanagisawa, Phys. Stat. Sol. a 11 (1972) 581.
[41] M. Chevreton, M. Murat, E.F. Bertaut, Centre Nat. Rech. Scient., Paris, 1967, p. 49.
[42] M. Yamaguchi, T. Hashimoto, J. Phys. Soc. Jpn. 32 (1972) 635.
[43] V. Carteaux, D. Brunet, G. Ouvrard, G. Andre, J. Phys.: Condens. Matter 7 (1995) 69.
[44] M. Yuzuri, M. Narita, T. Kaneko, S. Abe, H. Yoshida, J. Phys. Coll. C8 (Suppl. 12) (1988) 233.
[45] S. Ohta, T. Kanomata, T. Kaneko, H. Yoshida, J. Phys.: Condens. Matter. 5 (1993) 2759.
[46] S. Ohta, Y. Adachi, T. Kaneko, M. Yuzuri, H. Yoshida, J. Phys. Soc. Jpn. 63 (1994) 2225.
[47] V.A. Gordienko, V.V. Zubenko, V.I. Nikolaev, Sov. Phys. JETP 30 (1970) 864.
[48] H. Ido, K. Shirakawa, T. Suzuki, T. Kaneko, J. Phys. Soc. Jpn. 26 (1969) 663.
[49] M. Yuzuri, T. Kanomata, T. Kaneko, J. Magn. Magn. Mater. 70 (1987) 223.